Impacts of central Pacific and eastern Pacific El Niños on tropical cyclone tracks over the western North Pacific

Chi-Cherng Hong,[1] Yuan-Hsing Li,[1] Tim Li,[2] and Ming-Ying Lee[3]

Received 7 July 2011; revised 27 July 2011; accepted 27 July 2011; published 30 August 2011.

[1] This study examines the different impacts of two types of El Niños, the eastern Pacific El Niño (EP-EN) and the central Pacific El Niño (CP-EN), on tropical cyclone (TC) tracks over the western North Pacific (WNP) based on observational data. Whereas TC tracks between CP-EN and EP-EN show a small difference in boreal summer (JJA), they do exhibit a great difference in boreal autumn (SON), that is, TCs recurve northward at a further westward location near the coastline of East Asia during CP-EN. As a consequence, more TCs make landfall to Taiwan and South China during CP-EN. A further observational analysis indicates that the westward shift of the subtropical high and associated steering flow during CP-EN is a key factor that causes the difference in the TC tracks in autumn. Numerical experiments further suggest that the difference of local SST in the WNP between CP-EN and EP-EN accounts for the distinctive differences in the local Hadley circulation, the subtropical high and the TC steering flow. **Citation:** Hong, C.-C., Y.-H. Li, T. Li, and M.-Y. Lee (2011), Impacts of central Pacific and eastern Pacific El Niños on tropical cyclone tracks over the western North Pacific, *Geophys. Res. Lett.*, *38*, L16712, doi:10.1029/2011GL048821.

1. Introduction

[2] Tropical cyclone (TC) activity over the western North Pacific (WNP) varies from year to year, partially due to the mean circulation change associated with the remote influence of the El Niño–Southern Oscillation (ENSO). For example, TC genesis number increases over the southeastern (northwestern) quadrant of the WNP during El Niño (La Niña) developing summer [e.g., *Chan*, 2000; *Chia and Ropelewski*, 2002; *Wang and Chan*, 2002; *Wu et al.*, 2004; *Camargo and Sobel*, 2005]. Recent studies suggested that the El Niño can be separated into two types, the central Pacific El Niño (CP-EN) and the eastern Pacific El Niño (EP-EN), based on the zonal location of a maximum sea surface temperature anomaly (SSTA) at the equator [e.g., *Kug et al.*, 2009; *Kao and Yu*, 2009]. It was shown that the two types of El Niños exert different impacts on the TC frequency over the North Atlantic and Pacific [*Kim et al.*, 2009, 2011; *Chen and Tam*, 2010]. TC frequency over the WNP during CP-EN developing phase is significantly higher than that during EP-EN developing phase. It was further found that such an impact is season-dependent [*Chen and Tam*, 2010], that is, the difference is only significant during boreal summer (JJA) but insignificant in boreal autumn (SON).

[3] It was argued that the increase of TC genesis number over the WNP during CP-EN developing summer (JJA) is attributed to the westward shift of El Nino induced Gill-type low-level cyclonic circulation response, which strengthens the WNP monsoon trough and provides a favorable large-scale environment for TC genesis [*Chen and Tam*, 2010]. Whereas the impact of the two type El Niños on TC frequency was well explored, their influence on TC tracks is not clear. In this study we intend to reveal the possible impact of the two types of El Niños on TC track in the WNP. We will focus on the changes of the WNP subtropical high (SH) and the steering flow in association with the two type El Niños. Numerical model experiments are further conducted to understand the possible mechanism through which the two type El Niños affect TC track in the WNP.

2. Data and Methodology

[4] The best-track dataset (including 6 hourly TC position and intensity) from the Joint Typhoon Warning Center (JTWC) for the period of 1965–2009 is used to analyze the TC's frequence and track density. The main paths of TC tracks are plotted by tracing the local maximum of TC track density, following *Wu et al.* [2005]. The definition of the central Pacific and eastern Pacific El Niños follows *Kim et al.* [2011]. Six EP-EN events (1965, 1972, 1976, 1982, 1987, 1997) and six CP-EN events (1991, 1994, 2002, 2004, 2006, and 2009) are selected for composite analyses. Monthly atmospheric datasets of NCEP/NCAR Reanalysis I [*Kalnay et al.*, 1996], the SST from Met Office Hadley Centre's sea ice and sea surface temperature [*Rayner et al.*, 2003], and the outgoing longwave radiation (OLR) [*Liebmann and Smith*, 1996] are used for diagnosing large-scale circulation anomalies. An atmospheric general circulation model, ECHAM5 [*Roeckner et al.*, 2003] with a horizontal resolution of T42 and 19 vertical sigma levels, is used for numerical modeling experiments. A series of 6-member ensemble simulations were conducted for a period of one year, with the initiation condition from 1 January. In the control experiment, the model is forced by the observed monthly climatological SST. Two additional numerical experiments, Global-exp and WNP-exp, were further conducted by superposing the observed global monthly SSTA pattern (CP-EN minus EP-EN) and the local SSTA pattern in WNP into the monthly climatological SST field respectively.

3. Results

3.1. Observed TC Track Difference Associated With CP-EN and EP-EN

[5] The comparison of TC genesis frequency over the WNP between the two type El Niños is shown in Figures 1a and 1b. While the climatologic mean number is 12.6, the

[1]Department of Science/Earth and Life, Taipei Municipal University of Education, Taipei, Taiwan.
[2]IPRC, SOEST, University of Hawaii at Manoa, Honolulu, Hawaii, USA.
[3]Central Weather Bureau, Taipei, Taiwan.

0094-8276/11/2011GL048821

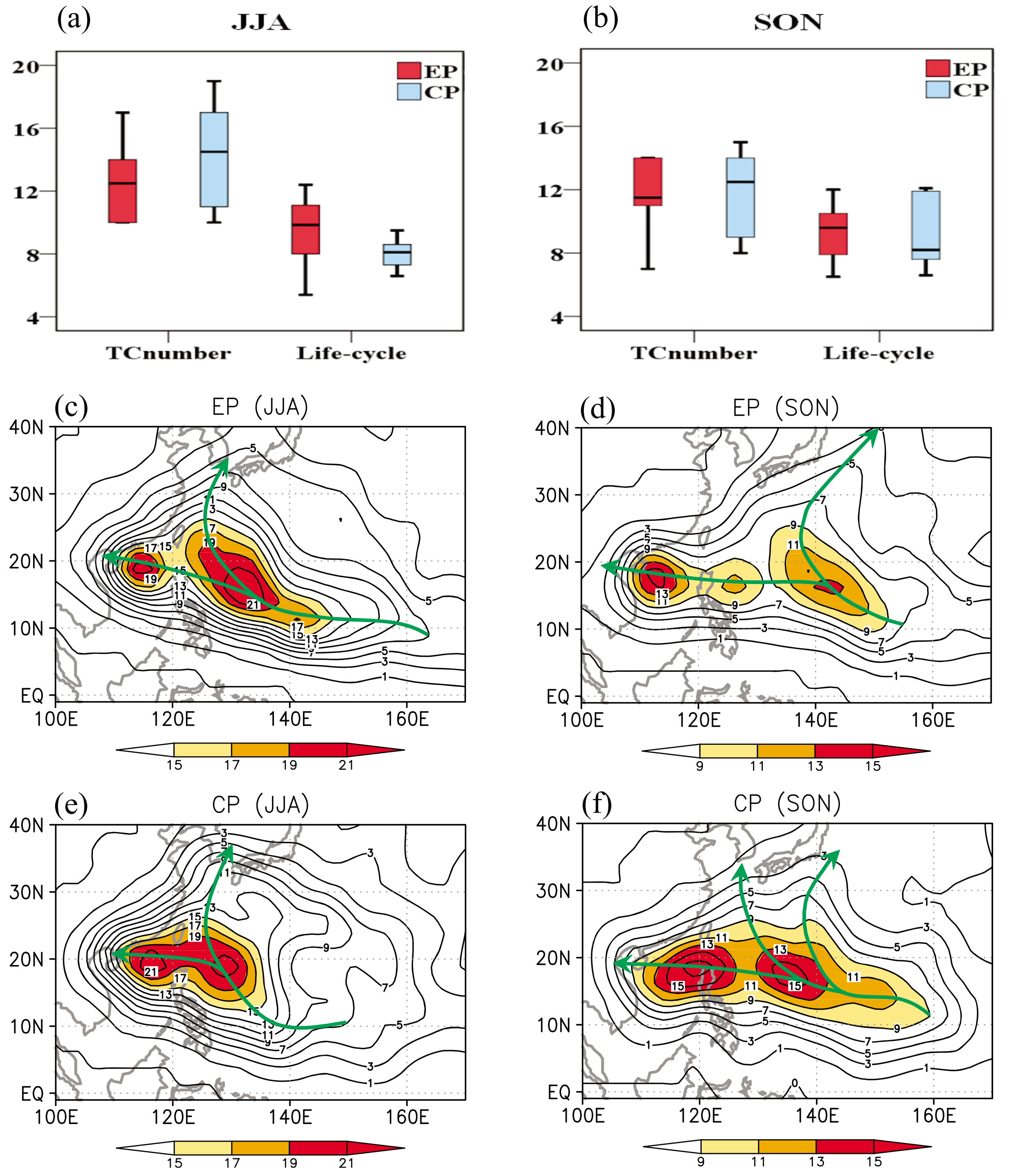

Figure 1. The comparison of the box-and whisker plot of TC frequency and life cycle in the WNP during (a) JJA, and (b) SON between EP-EN and CP-EN. The box-and whisker plot (from bottom to top) denotes the minimum, quartile 1 (Q1), mean, quartile 3 (Q3), and maximum. The bar (Q3-Q1) is equivalent to the variation. (c–f) Same as in Figures 1a and 1b, but for the track density (TC frequency in each 2.5° × 2.5° grid box) during (left) JJA and (right) SON. The thick green arrows denote the main paths of TC tracks.

average TC number during CP-EN is 14.3 in JJA, which is greater than that during EP-EN (12.7). The difference of TC frequency in boreal autumn (SON), however, is insignificant, consistent with *Chen and Tam* [2010].

[6] A further diagnosis shows that the TC genesis location during EP-EN is extended further to the east, in consistence with the eastward extension of the WNP monsoon trough (Figure 1c and Figure S1 in the auxiliary material).[1] This modulation of the monsoon trough leads to a longer TC

[1]Auxiliary materials are available in the HTML. doi:10.1029/2011GL048821.

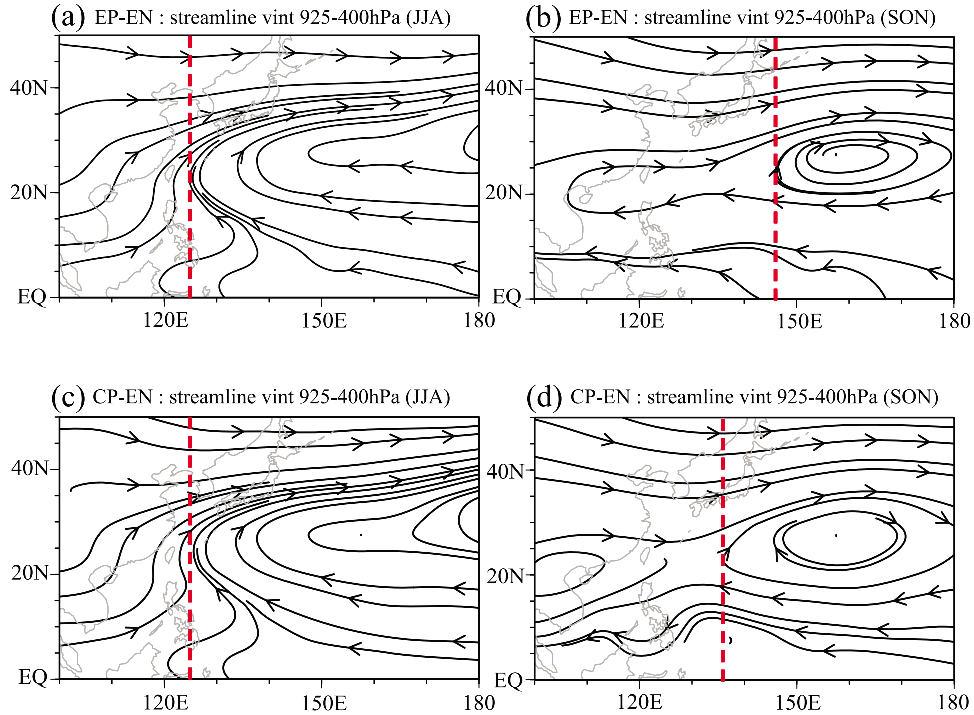

Figure 2. (a–d) Same as in Figures 1c–1f, but for the steering flow. The steering flow is defined as the vertical integrated streamline from 925 hPa to 400 hPa. The red dashed red lines indicate the west edge of the steering flow during SON.

lifecycle of EP-EN (~9.4 days) in JJA compared to that of CP-EN (~8 days).

[7] The comparison of TC tracks between EP-EN and CP-EN is shown in Figures 1e and 1f. TC tracks may be separated into two main paths, a westward track and a northward recurving track (denoted by green arrows). For the westward track, both type El Ninos show a similar path in JJA and SON, except that the path during EP-EN in JJA can be traced back further to the east (around 170°E) due to the eastward extension of TC genesis location (Figure S1). For the northward recurving track, there is no significant difference between CP-EN and EP-EN in JJA, whereas it exhibits a marked difference in northward recurving location during SON. The major difference arises from the fact that the maximum TC density in the WNP shifts westward from 142°E to 135°E and that the northward recurving TC tracks can be further separated into two main paths during CP-EN (Figures 1d and 1f). A t-test confirms that the difference of the northward recurving TC tracks during SON between CP-EN and EP-EN is statistically significant (Figure S2). It is interesting to note that there are also two main northward recurving TC paths in the work by *Wu et al.* [2005, see Figure 1]. Because TCs tend to recurve at a further westward location, more TCs make landfall to Taiwan and South China during CP-EN.

[8] As TC track over the WNP is primarily controlled by the steering flow (e.g., *Ho et al.*, 2004), we examine the vertically integrated (925–400 hPa) mean flow change associated with CP-EN and EP-EN. It is interesting to note that the steering flow does not exhibit a significant difference during JJA between EP-EN and CP-EN (Figures 2a and 2c), that is, the northward recurving longitudinal location (~130°E) is quite similar. This is consistent with the TC track characteristic shown in Figure 1. In contrast, the steering flow in SON exhibits a marked difference between EP-EN and CP-EN (Figures 2b and 2d), with the averaged northward recurving longitudinal location shifting westward during CP-EN. The change of the steering flow is consistent with the change of the SH. The contour lines of the 5880 m (thick black line) at 500 hPa clearly reflects this difference: while the SH retreats eastward to central Pacific for both type El Niños in boreal autumn, such an eastward retreat is greater during EP-EN (Figure S3). This is again consistent with the fact that TC northward recurving appears at a further westward location during CP-EN compared with that during EP-EN.

3.2. Role of the Local SST Warming in the TC Track Difference

[9] In this section, we propose a possible mechanism responsible for the TC track change in SON. We argue that the local SSTA over the WNP plays a role in causing the SH and steering flow differences between the two type El Niños. Figure 3 shows the SSTA difference between CP-EN and EP-EN during SON. A negative SSTA appears over the equatorial eastern Pacific and a positive SSTA occurs over the WNP. The OLR difference field shows enhanced tropical (suppressed) convection over the warm (clod) SSTA regions. The local warm SSTA and enhanced convection at 15°N may enhance the local Hadley cell, which in turn strengthens subsidence at subtropics (~25°N) (Figure 3b). Note that this local Hadley cell anomaly can only be identified during SON. The enhanced subsidence may further dry the troposphere and cause the westward extension of the SH [*Sui et al.*, 2007; *Chung et al.*, 2011]. The result above suggests that the westward shift of the SH and the steering

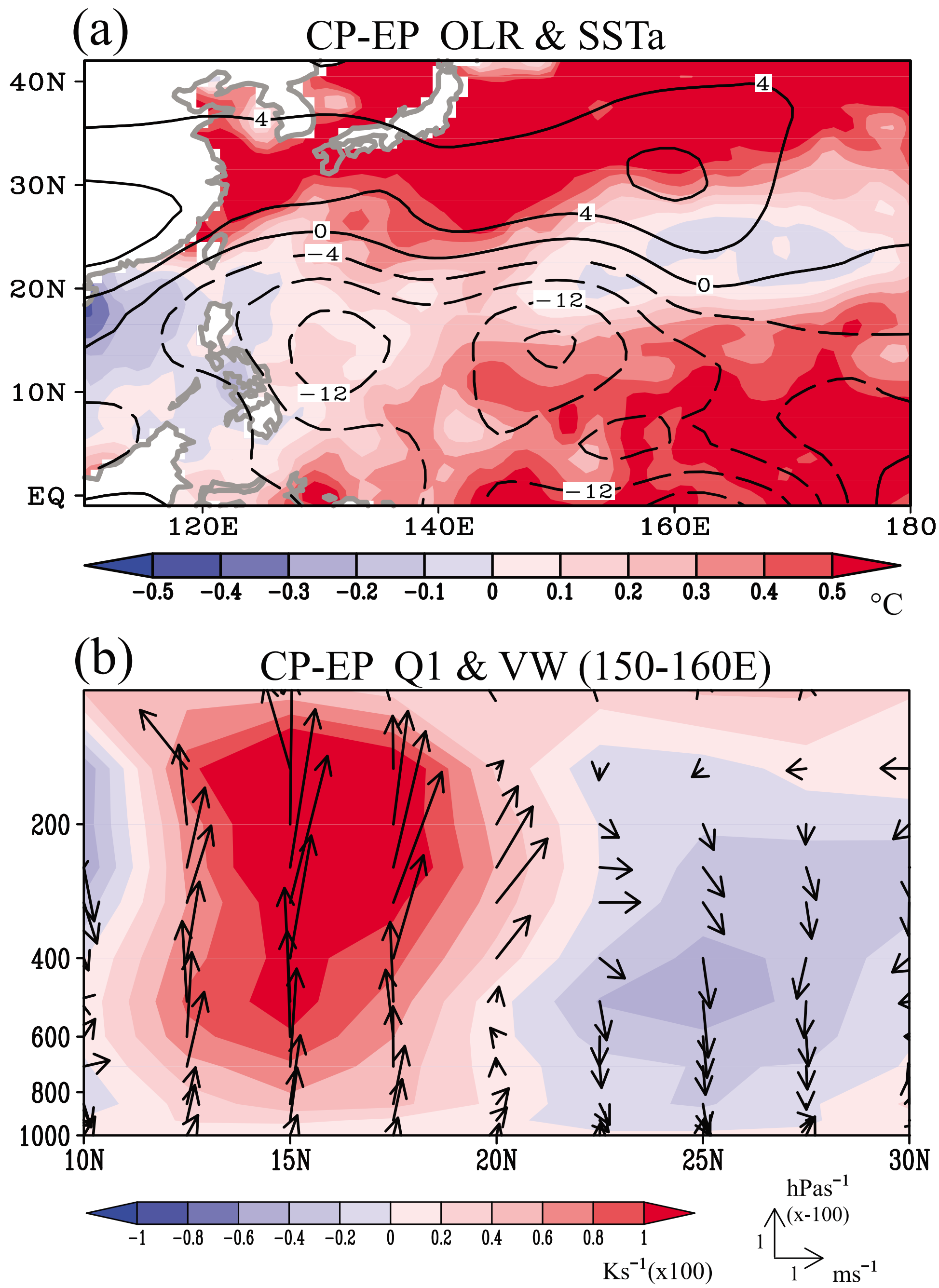

Figure 3. (a) The difference of the composite SSTA (shading) and OLR anomaly (contour, interval 4 Wm^{-2}) between CP-EN and EP-EN (CP-EN minus EP-EN) during SON. (b) Same as in Figure 3a but for the local Hadley circulation (averaged over 150–160°E, 130–160°E shows the similar results) and apparent heat source (Q1, *Yani and Chu*, 1973, shaded) anomalies. The Q1 (unit: Ks^{-1}) and the vertical velocity (unit: hPa s^{-1}) had been multiplied by 100 and −100 respectively.

flow during CP-EN is likely associated with the warmer local SSTA over the WNP.

[10] To further explore the possible role of the local SSTA in causing the SH difference, two sets of ECHAM5 experiments, Global-exp and WNP-exp, were conducted. The details of numerical experiments were described in section 2. A local anomalous Hadley circulation is well simulated over the WNP (Figure 4a), with the anomalous ascending (descending) branch located at 10–15°N (25–30°N), consistent with the observed. The numerical result suggests that the local meridional overturning circulation and associated SH change is closely related with the SSTA forcing. As both the local and remote SSTA may contribute to the circulation anomaly over the WNP, we further conducted an additional experiment in which only the local SSTA was specified (Figure 4d). A similar local Hadley circulation anomaly is reproduced in this case (Figure 4c), suggesting that the SSTA over the WNP plays a dominant role in affecting the local Hadley circulation change. A further sensitivity experiment showed that the contribution of the

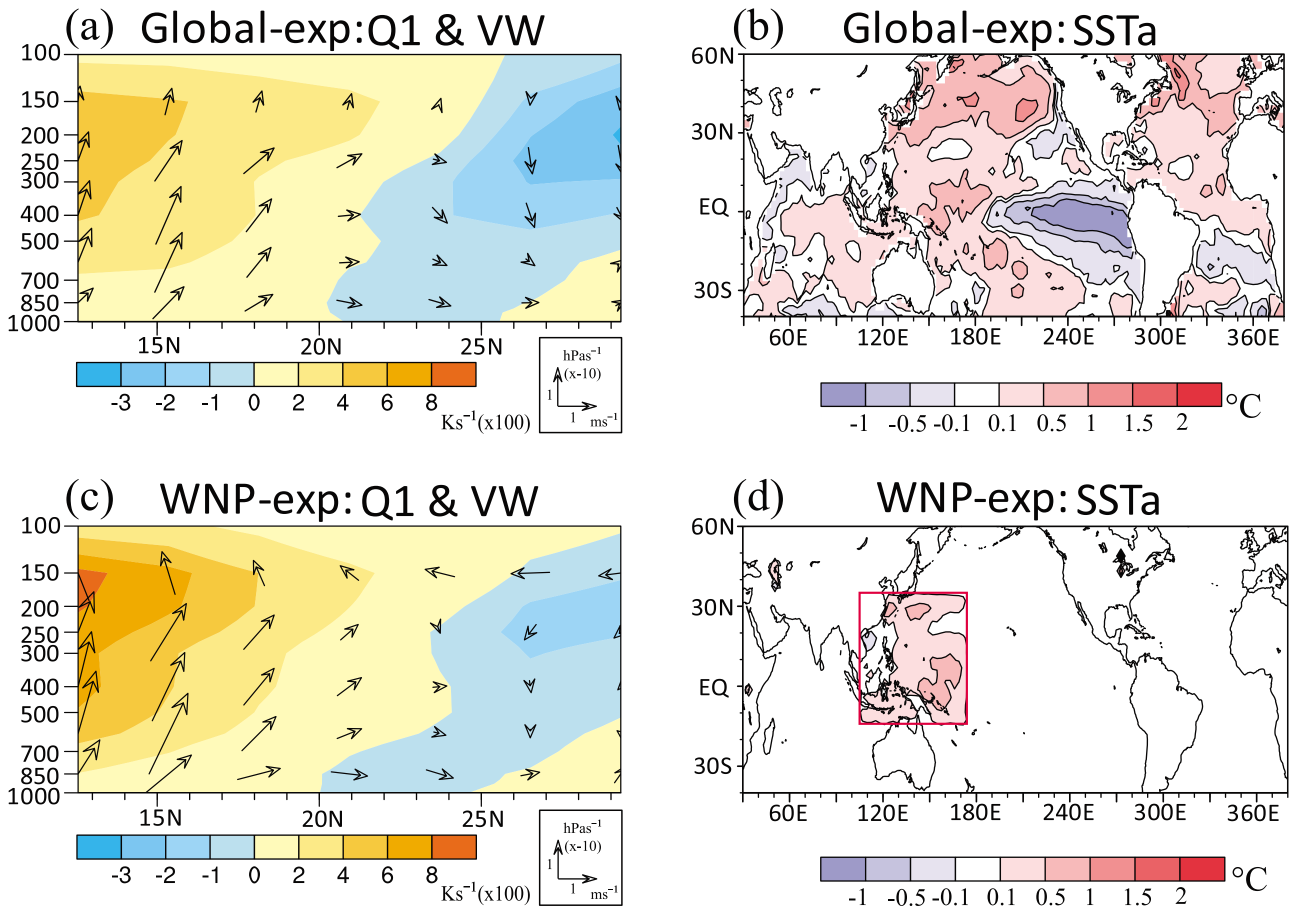

Figure 4. (a) The same as in Figure 3b but for the responses in ECHAM5 to a prescribed (b) global SSTA pattern (CP-EN minus CP-EN). (c, d) Same as in Figures 4a and 4b except for the response to a specified local SSTA pattern in the WNP.

equatorial eastern Pacific SSTA is weak (not shown). Thus, both the observational analysis and numerical experiments point out that the local warm SSTA and associated circulation changes over the WNP are responsible for the different TC tracks in northern fall between CP-EN and EP-EN.

4. Conclusion and Remarks

[11] The different impacts of the central Pacific and eastern Pacific El Niños on TC tracks in the WNP and possible mechanism responsible for the difference are investigated based on the observational analysis and numerical experiments. The main results are summarized as the followings:

[12] 1. In boreal summer (JJA), while TC frequency during CP-EN is greater than that during EP-EN, the difference in TC track over the WNP between the two type El Niños is small. In boreal autumn (SON), on the other hand, TC track exhibits a great difference between CP-EN and EP-EN, but TC frequency is nearly the same.

[13] 2. The difference of autumn TC track between the two type El Niños is primarily attributed to the modulation of the SH and associated steering flow. Both the steering flow and the SH during CP-EN exhibit a westward shift compared to those during EP-EN. This results in the northward TC recurving at a further westward location near the coastline of East Asia during CP-EN and more TC landfall in Taiwan and South China.

[14] 3. Numerical experiments suggest that the local warmer SSTA in the WNP during CP-EN plays an important role in modulating the local Hadley circulation, the SH and the steering flow compared to EP-EN. The influence of the equatorial eastern Pacific SSTA is relatively weak.

[15] The result above has some implication for future TC activity in the WNP. It has been shown that the frequency of CP-EN tends to increase under global warming [*Yeh et al.*, 2009]. This implies that more typhoons may hit Taiwan and South China in future warming climate. On the other hand, the analysis of two high-resolution global model outputs by *Li et al.* [2010] showed that the TC number in the WNP will decrease significantly under global warming. The two factors (track change versus frequency change) offset each other. As a result, it will be difficult to project the future change of landfall typhoons in the East Asia coasts. Further observational and modeling studies are needed in order to understand and reveal the regional characteristics of future TC projection in the WNP.

[16] **Acknowledgments.** Comments of two anonymous reviewers are highly appreciated. The authors thank H.-H. Chia for discussions. CCH was supported by NSC 99-2628-M133-001 and NSC 100-2111-M-133-001. TL was supported by ONR grants N000140810256 and N000141010774 and by the International Pacific Research Center that is sponsored by the Japan Agency for Marine-Earth Science and Technology (JAMSTEC), NASA (NNX07AG53G) and NOAA (NA17RJ1230). This is SOEST contribution 8382 and IPRC contribution 808.

[17] The Editor thanks the two anonymous reviewers for their assistance in evaluating this paper.

References

Camargo, S. J., and A. H. Sobel (2005), Western North Pacific tropical cyclone intensity and ENSO, *J. Clim.*, *18*, 2996–3006, doi:10.1175/JCLI3457.1.

Chan, J. C. L. (2000), Tropical cyclone activity over the western North Pacific associated with El Niño and La Niña events, *J. Clim.*, *13*, 2960–2972, doi:10.1175/1520-0442(2000)013<2960:TCAOTW>2.0.CO;2.

Chen, G., and C. Y. Tam (2010), Different impacts of two kinds of Pacific Ocean warming on tropical cyclone frequency over the western North Pacific, *Geophys. Res. Lett.*, *37*, L01803, doi:10.1029/2009GL041708.

Chia, H. H., and C. F. Ropelewski (2002), The interannual variability in the genesis location of tropical cyclones in the northwest Pacific, *J. Clim.*, *15*, 2934–2944, doi:10.1175/1520-0442(2002)015<2934:TIVITG>2.0.CO;2.

Chung, P.-H., C.-H. Sui, and T. Li (2011), Interannual relationships between the tropical SST and summertime subtropical anticyclone over the western North Pacific, *J. Geophys. Res.*, *116*, D13111, doi:10.1029/2010JD015554.

Ho, C. H., J. J. Baik, J. H. Kim, D. Y. Gong, and C. H. Sui (2004), Interdecadal changes in summertime typhoon tracks, *J. Clim.*, *17*, 1767–1776, doi:10.1175/1520-0442(2004)017<1767:ICISTT>2.0.CO;2.

Kalnay, E., et al. (1996), The NCEP/NCAR 40-year reanalysis project, *Bull. Am. Meteorol. Soc.*, *77*, 437–471, doi:10.1175/1520-0477(1996)077<0437:TNYRP>2.0.CO;2.

Kao, H. Y., and J. Y. Yu (2009), Contrasting eastern Pacific and central Pacific types of ENSO, *J. Clim.*, *22*, 615–631, doi:10.1175/2008JCLI2309.1.

Kim, H. M., P. J. Webster, and J. A. Curry (2009), Impact of shifting patterns of Pacific Ocean warming on North Atlantic tropical cyclones, *Science*, *325*, 77–80, doi:10.1126/science.1174062.

Kim, H. M., P. J. Webster, and J. A. Curry (2011), Modulation of North Pacific tropical cyclone activity by three phases of ENSO, *J. Clim.*, *24*, 1839–1849, doi:10.1175/2010JCLI3939.1.

Kug, J.-S., F.-F. Jin, and S.-I. An (2009), Two types of El Niño Events: Cold tongue El Niño and warm pool El Niño, *J. Clim.*, *22*, 1499–1515, doi:10.1175/2008JCLI2624.1.

Li, T., M. Kwon, M. Zhao, J. Kug, J. Luo, and W. Yu (2010), Global warming shifts Pacific tropical cyclone location, *Geophys. Res. Lett.*, *37*, L21804, doi:10.1029/2010GL045124.

Liebmann, B., and C. A. Smith (1996), Description of a complete (interpolated) outgoing longwave radiation dataset, *Bull. Am. Meteorol. Soc.*, *77*, 1275–1277.

Rayner, N. A., D. E. Parker, E. B. Horton, C. K. Folland, L. V. Alexander, D. P. Rowell, E. C. Kent, and A. Kaplan (2003), Global analyses of sea surface temperature, sea ice, and night marine air temperature since the late nineteenth century, *J. Geophys. Res.*, *108*(D14), 4407, doi:10.1029/2002JD002670.

Roeckner, E., et al. (2003), The atmospheric general circulation model ECHAM5, Part I: Model description, *Rep. 349*, 127 pp., Max Planck Inst. for Meteorol, Hamburg, Germany.

Sui, C.-H., P.-H. Chung, and T. Li (2007), Interannual and interdecadal variability of the summertime western north Pacific subtropical high, *Geophys. Res. Lett.*, *34*, L11701, doi:10.1029/2006GL029204.

Wang, B., and J. C. L. Chan (2002), How strong ENSO events affect tropical storm activity over the western North Pacific, *J. Clim.*, *15*, 1643–1658, doi:10.1175/1520-0442(2002)015<1643:HSEEAT>2.0.CO;2.

Wu, L., B. Wang, and S. Geng (2005), Growing typhoon influence on East Asia, *Geophys. Res. Lett.*, *32*, L18703, doi:10.1029/2005GL022937.

Wu, M. C., W. L. Chang, and W. M. Leung (2004), Impacts of El Niño Southern Oscillation events on tropical cyclone landfalling activity in the western North Pacific, *J. Clim.*, *17*, 1419–1428, doi:10.1175/1520-0442(2004)017<1419:IOENOE>2.0.CO;2.

Yani, M. S. E., and J. H. Chu (1973), Determination of bulk properties of tropical cloud clusters from large-scale heat and moisture budgets, *J. Atmos. Sci.*, *30*, 611–627, doi:10.1175/1520-0469(1973)030<0611:DOBPOT>2.0.CO;2.

Yeh, S.-W., J.-S. Kug, B. Dewitte, M.-H. Kwon, and B. P. Kirtman (2009), El Niño in a changing climate, *Nature*, *461*, 511–514, doi:10.1038/nature08316.

C.-C. Hong and Y.-H. Li, Department of Science/Earth and Life, Taipei Municipal University of Education, 1 Ai Kuo West Rd., Taipei 10048, Taiwan. (cchong@tmue.edu.tw; hong0202@gmail.com)

M.-Y. Lee, Central Weather Bureau, 64, Gongyuan Rd., Taipei 10048, Taiwan.

T. Li, IPRC, SOEST, University of Hawaii at Manoa, 2525 Correa Rd., Honolulu, HI 96822, USA.